

# Entropy-Based Space Object Data Association Using an Adaptive Gaussian Sum Filter

Daniel R. Giza\*, Puneet Singla†, John L. Crassidis‡, Richard Linares§, Paul J. Cefola¶

*University at Buffalo, State University of New York, Amherst, NY, 14260-4400*

Keric Hill||

*Pacific Defense Solutions, 1300 N. Holocono Street, Suite 116, Kihei, HI, 96753*

**This paper shows an approach to improve the statistical validity of orbital estimates and uncertainties as well as a method of associating measurements with the correct resident space objects and classifying events in near realtime. The approach involves using an adaptive Gaussian mixture solution to the Fokker-Planck-Kolmogorov equation for its applicability to the resident space object tracking problem. The Fokker-Planck-Kolmogorov equation describes the time-evolution of the probability density function for nonlinear stochastic systems with Gaussian inputs, which often results in non-Gaussian outputs. The adaptive Gaussian sum filter provides a computationally efficient and accurate solution for this equation, which captures the non-Gaussian behavior associated with these nonlinear stochastic systems. This adaptive filter is designed to be scalable, relatively efficient for solutions of this type, and thus is able to handle the nonlinear effects which are common in the estimation of resident space object orbital states. The main purpose of this paper is to develop a technique for data association based on entropy theory that is compatible with the adaptive Gaussian sum filter. The adaptive filter and corresponding measurement association methods are evaluated using simulated data in realistic scenarios to determine their performance and feasibility.**

## I. Introduction

Recent events in space, including the collision of Russia's Cosmos 2251 satellite with Iridium 33 and China's Feng Yun 1C anti-satellite demonstration, have stressed the capabilities of Space Surveillance Network (SSN), its associated tracking sensors, orbit estimators and analysis tools. The SSN continuously tracks more than 18,000 resident space objects (RSOs) and debris at any given time providing critical collision avoidance warnings not only to military and NASA systems but to commercial systems as well. The information on the RSOs is stored in a catalog. However, because of the large number of RSOs and the limited number of sensors available to track these objects, it is impossible to maintain persistent surveillance on all objects. Therefore there is inherent uncertainty and latency in the catalog. The rapid estimation of the orbit and identity of RSOs and the accurate assessment of confidence in those estimates will be a significant improvement particularly for the space situational awareness (SSA) community and the warfighter. The near-real time detection of RSO maneuvers for collision avoidance directly affects the protection of space assets, as the recent Iridium satellite collision illustrates. Here an unexpected maneuver placed a satellite

---

\*Graduate Student, Department of Mechanical & Aerospace Engineering. Email: drgiza@buffalo.edu, Student Member AIAA.

†Assistant Professor, Department of Mechanical & Aerospace Engineering. Email: psingla@buffalo.edu, Senior Member AIAA.

‡Professor, Department of Mechanical & Aerospace Engineering. Email: johnc@buffalo.edu, Associate Fellow AIAA.

§Graduate Student, Department of Mechanical & Aerospace Engineering. Email: linares2@buffalo.edu, Student Member AIAA.

¶Adjunct Professor, Department of Mechanical & Aerospace Engineering. Email: paul.cefola@gmail.com, Associate Fellow AIAA.

||Senior Scientist. Email: kerichill@pacificds.com, Member AIAA.

into an orbit which resulted in a collision. Responsive, near real-time algorithms which are based on accurate uncertainty information have the potential to rapidly detect changes in orbital state by comparing observations to the estimated state and uncertainty. This would enable faster sensor response and collision risk assessment.

Effective SSA requires more than just estimating locations or collecting images of RSOs. It is the ability to identify a satellite's capabilities and predict future operations and performance limits with known confidence. The challenge lies in bringing together limited measurements from multiple sensors, sensor management, and computationally efficient uncertainty characterization methods to deliver to decision makers the capability to assess a situation in terms of threat and/or impact in a timely manner. Currently, intervals between orbit updates for RSOs can be 24 hours or longer and decisions are made without accurate knowledge of the uncertainty in the orbit estimates. Realtime orbit estimation, object identification, and event classification would allow the warfighter to respond to threats quickly, while accurate uncertainty information would allow the warfighter to respond appropriately.

While there are many established sequential estimators that can perform realtime orbit estimation and provide the associated covariance, the RSO tracking problem presents special difficulties. The current estimation technique tends to be applied with limited tracking data for a wide variety of orbit regimes when there is little or no information included in the estimation process on the RSO mass, shape, radiative properties or attitude. In addition, it is likely that the uncertainty distribution for many RSOs is not Gaussian and cannot be represented accurately by a covariance matrix that has been developed with an assumed Gaussian probability density function (pdf).

The most common method for representing orbital uncertainty is to approximate the initial distribution using a Gaussian model and use linear error theory to propagate the mean and covariance of the Gaussian model forward in time. This can lead to significant errors when propagating uncertain orbits for large amounts of times.<sup>1,2</sup> In addition to this approach, several approximate techniques exist in the literature to approximate the initial condition uncertainty evolution, the most popular being Sequential Monte Carlo (SMC) methods,<sup>3</sup> Gaussian closure,<sup>4</sup> Equivalent Linearization,<sup>5</sup> and Stochastic Averaging.<sup>6</sup> All of these algorithms, except Monte Carlo methods, are similar in several respects and are suitable only for linear or moderately nonlinear (quasi-linear) systems because the effect of neglected higher-order terms can lead to significant errors. Monte Carlo methods require extensive computational resources and become increasingly infeasible for high-dimensional dynamic systems.<sup>7</sup> Furthermore, all these approaches provide only an approximate description of the uncertainty propagation problem by restricting the solution to a small number of parameters, for instance the first  $N$  moments of the sought pdf.

For stochastic continuous dynamic systems the exact evolution of the state pdf is given by the Fokker-Planck-Kolmogorov Equation (FPKE).<sup>8</sup> Park et al.<sup>9</sup> have discussed the use of the FPKE to analyze the spacecraft trajectory statistics by incorporating higher-order Taylor series terms in the spacecraft dynamics. Analytical solutions for the FPKE exist only for a stationary probability density function and are restricted to a limited class of dynamical systems.<sup>8,10</sup> Recently Terejanu et al. have developed an Adaptive Gaussian Sum filter (AGSF) approach<sup>11,12</sup> for accurate uncertainty propagation through nonlinear dynamical systems while incorporating the solution to the FPKE. This approach has been successfully applied to propagate initial orbit uncertainty through a low-Earth orbit with nonconservative atmospheric drag<sup>13</sup> and has also been applied to the spacecraft attitude estimation problem.<sup>14,15</sup>

Data association (DA) involves the matching of sensor measurements to specific tracks or targets. The need for an effective DA algorithm has been mentioned previously. If measurement-to-target matching fails, proper state estimation will be impossible. Nearest Neighbor (NN) is the simplest DA algorithm, used for single target tracking. When multiple measurements fall within a target's validation gate, the one that is closest with respect to a pre-defined distance measure is assumed to come from that target. Sometimes called the optimal assignment approach, global nearest neighbor (GNN) is the multi-target version of the NN approach. Instead of minimizing a single distance, GNN looks to minimize a global distance measure. Two assumptions are made: 1) each measurement can only be associated to one track, and 2) each track can only be associated with one measurement.

Unlike the DA algorithms, Joint Probabilistic Data Association (JPDA) does not associate each measurement with a specific track. Instead, a probability for measurement-to-target association is calculated for each measurement within a target's validation gate. Karlsson and Gustafsson<sup>16</sup> propose a Monte Carlo approach to JPDA. Instead of assigning a measurement-to-estimate probability, a measurement-to-particle-cloud probability is computed. Four filter-DA combinations are simulated: Particle Filter (PF) with Monte

Carlo JPDA, PF with NN association, Extended Kalman Filter (EKF) with JPDA, and EKF with NN association. Two targets are present, each moving in straight-line paths that cross at one point. A root-mean-square-error analysis is performed over sixty simulations. For both filters, the JPDA outperformed the NN association. The PF was superior with the JPDA, while the converse was true for the NN association.

Frank et al.<sup>17</sup> examine two different filters based on combining the PF with the JPDA algorithm. Each filter uses a different assumption: 1) the states of the targets conditioned on past measurements are mutually independent [this is termed the Independent Sample Based Joint Probabilistic Data Association Filter (ISBJPDAF)], and 2) the states of the targets conditioned on past measurements are correlated [this is termed the Coupled Sample Based Joint Probabilistic Data Association Filter (CSBJPDAF)]. Another combination of the particle filter with a JPDA filter is shown by Vermaak et al.<sup>18</sup> Their algorithm is referred to as the Monte Carlo Joint Probabilistic Data Association Filter (MCJPDAF). Association uncertainty is dealt with by combining all feasible hypotheses according to their corresponding posterior probabilities. These values are computed using Monte Carlo samples. This produces a more accurate probabilistic description compared to the Gaussian one that is produced by a standard JPDAF.

In recent years, PFs have been receiving more of a focus in literature. Hue et al.<sup>19</sup> investigated the applicability of using PFs to multiple target tracking. One of the advantages of this type of approach is that it is highly effective at handling nonlinear models and non-Gaussian noise. In this paper, the classical PF is combined with a Gibbs sampler-based estimation of the assignment probabilities. Two assumptions are made: 1) a given measurement can originate from either one target, or from clutter, and 2) a given target can produce one or more measurements during each scan. One of the differences between this algorithm and that of the Probabilistic Multiple Hypothesis Tracking (PMHT) and JPDA is that the former does not require a priori knowledge of the probability of detecting a target. The simplest method proposed involves measurements from a single sensor of a fixed number of targets. This is then extended to a varying number of targets, and lastly to a scenario with multiple sources of measurements.

Although PF-based methods are highly useful for data association involving non-Gaussian problems, which are typical for RSO tracking, they have the significant disadvantage of being computationally expensive. This is because PFs are based on Monte Carlo sampling approaches. Even though methods have been proposed to reduce the computational load, such as replacing the standard importance sampling with a Markov Chain Monte Carlo (MCMC) method,<sup>20</sup> they generally are still not viable for actual RSO tracking applications. As illustrated in Refs. [11–13, 15], the AGSF algorithm can produce the entire non-Gaussian pdf with much less computations than what is typically required in particle filters. To develop a successively refining pdf representation, it is important to define a metric for the data association error, so that improvement due to refinements can be assessed. In this paper the metric for modeling error in terms of *information geometry* is defined while making use of the Kullback-Leibler (KL) divergence measure.

The combination of the AGSF with an entropy-based approach for data association is well suited for orbit problems where the errors may be highly non-Gaussian. Current methods, such as particle filters, that reproduce the entire pdf are computationally expensive in general. Also, most DA algorithms for orbit estimation problems are based on Gaussian models, which can provide inaccuracies when non-Gaussian conditions exist. The main advantages of the approach shown in this paper over existing approaches are: 1) it provides a computationally efficient approach which can be implementable in realtime using modern-day computers, and 2) it can work well for highly non-Gaussian problems.

The organization of this paper is as follows. First a review of the FPKE is provided. Then the AGSF is summarized followed by a review of entropy-based DA. A comparison is made using the entropy-based DA approach with an Unscented Kalman filter and the AGSF.

## II. The Fokker-Planck-Kolmogorov Equation (FPKE)

In conventional *deterministic* systems, the system state assumes a fixed value at any given instant of time. However, in stochastic dynamics it is a *random variable* and its time evolution is given by the following stochastic differential equation:

$$\dot{\mathbf{x}} = \mathbf{f}(t, \mathbf{x}) + \mathbf{g}(t, \mathbf{x})\Gamma(t), \quad \mathbf{x}(t_0) = \bar{\mathbf{x}}_0 \quad (1)$$

where  $\Gamma(t)$  represents a Gaussian white-noise process with the correlation function  $\mathbf{Q}\delta(t_1 - t_2)$  and  $\bar{\mathbf{x}}_0$  represents the nominal initial state. The uncertainty associated with the state vector  $\mathbf{x}(t) \in \mathbb{R}^n$  is usually characterized by a time parameterized state pdf,  $p(t, \mathbf{x})$ . In essence, the study of stochastic systems reduces

to finding the nature of the time-evolution of the system-state pdf (see Fig. 1) described by the FPKE:<sup>8</sup>

$$\begin{aligned} \frac{\partial}{\partial t} p(t, \mathbf{x}) &= \mathcal{L}_{FPK} p(t, \mathbf{x}) \\ &= \frac{\partial \mathbf{f}^T(t, \mathbf{x}) p(t, \mathbf{x})}{\partial \mathbf{x}} + \frac{1}{2} \text{Tr} \left( \mathbf{g}(t, \mathbf{x}(t)) \mathbf{Q} \mathbf{g}^T(t, \mathbf{x}(t)) \frac{\partial^2 p}{\partial \mathbf{x} \partial \mathbf{x}^T} \right) \end{aligned} \quad (2)$$

The FPKE is a formidable equation to solve, because of the following issues: 1) *Positivity* of the pdf, 2) *Normalization* constraint of the pdf:  $\int_{\mathbb{R}^n} p(t, \mathbf{x}) d\mathbf{x} = 1$ , & 3) *No fixed Solution Domain*: how to impose boundary conditions in a finite region and restrict numerical computation to regions where  $p > \sim 10^{-9}$ .

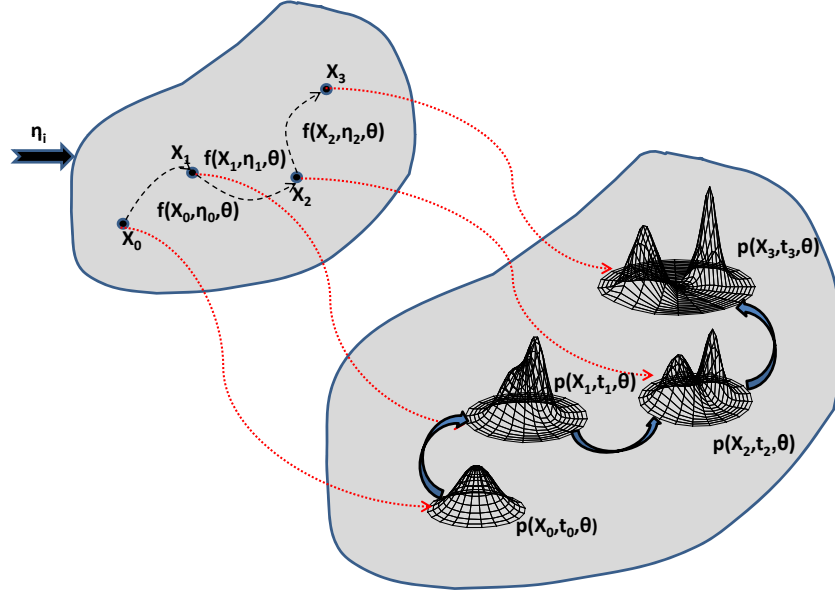


Figure 1. State and pdf Transition

Analytical solutions for the FPKE exist only for a stationary pdf and are restricted to a limited class of dynamical systems.<sup>8,10</sup> Thus researchers are actively looking at numerical approximations to solve the FPKE,<sup>21–25</sup> generally using the variational formulation of the problem. These traditional numerical approaches which discretize the space in which the pdf lies suffer from the “*curse of dimensionality*.” To overcome this obstacle, we will use a recently developed Adaptive Gaussian Sum Filter (AGSF) to accurately solve the FPKE. The key idea of the AGSF is to approximate the state pdf by a finite sum of Gaussian density functions whose mean and covariance are propagated from one time-step to the next using linear theory. The weights of the Gaussian kernels are updated at every time-step, by requiring the sum to satisfy the FPKE.<sup>11</sup> When properly formulated, the Gaussian mixture in the AGSF can be solved efficiently and accurately using convex optimization solvers, even if the mixture model includes many terms. This methodology effectively decouples a large uncertainty propagation problem into many small problems. As a consequence, the solution algorithm can be parallelized on most High Performance Computing (HPC) systems. Finally, a Bayesian framework can be used on the AGSF structure to assimilate (noisy) observational data with model forecasts.<sup>12</sup>

### A. Solution Using the AGSF

This subsection briefly summarizes the approach; details can be found in Refs. [11, 26, 27]. The Gaussian mixture model approximation (denoted by the caret  $\hat{\cdot}$ ) of the forecast pdf can be written as:

$$\hat{p}(t, \mathbf{x}(t)) = \sum_{i=1}^N w_i(t) \mathcal{N}(\mathbf{x}(t) \mid \boldsymbol{\mu}_i(t), \mathbf{P}_i(t)) \quad (3)$$

In this equation,  $\boldsymbol{\mu}_i(t)$  and  $\mathbf{P}_i(t)$  represent the mean and covariance of the  $i^{th}$  component of the Gaussian pdf,  $\mathcal{N}(\mathbf{x}(t) | \boldsymbol{\mu}_i(t), \mathbf{P}_i(t))$ , respectively, and  $w_i$  denotes the amplitude of  $i^{th}$  Gaussian in the mixture. The positivity and normalization constraint on  $\hat{p}(t, \mathbf{x})$  leads to the following conditions at every time-step:

$$\sum_{i=1}^N w_i(t) = 1 \text{ and } w_i(t) \geq 0, \forall i \quad (4)$$

In Ref. [28], it is shown that because all the components of the mixture pdf in Eq. (3) are Gaussian, only estimates of their mean and covariance need to be maintained. These estimates can be propagated using the linear system propagation methods such as the propagation part of the extended Kalman filter (EKF):

$$\dot{\boldsymbol{\mu}}_i(t) = \mathbf{f}(t, \boldsymbol{\mu}_i(t)) \quad (5)$$

$$\dot{\mathbf{P}}_i(t) = \mathbf{A}_i(t)\mathbf{P}_i(t) + \mathbf{P}_i(t)\mathbf{A}_i^T(t) + \mathbf{g}(t, \boldsymbol{\mu}_i(t))\mathbf{Q}(t)\mathbf{g}^T(t, \boldsymbol{\mu}_i(t)) \quad (6)$$

where  $\mathbf{A}_i(t) = \frac{\partial \mathbf{f}(t, \mathbf{x}_k)}{\partial \mathbf{x}} |_{\mathbf{x}=\boldsymbol{\mu}_i}$ . We mention that mean and covariance of each Gaussian component can also be propagated by using a continuous-time derivation of the Unscented Kalman Filter (UKF),<sup>29</sup> which uses a set of deterministically chosen sigma-points that capture the mean and covariance of the initial distribution. The propagation equations for mean and covariance are given as

$$\mathbf{X}_i = [\boldsymbol{\mu}_i \dots \boldsymbol{\mu}_i] + \sqrt{c}[\mathbf{0} \quad \mathbf{A} \quad -\mathbf{A}], \quad c = \alpha^2(n + \kappa) \quad (7)$$

$$\dot{\boldsymbol{\mu}}_i = \mathbf{f}(\mathbf{X}_i)\mathbf{w}_m \quad (8)$$

$$\dot{\mathbf{P}}_i = \mathbf{X}_i\mathbf{W}\mathbf{f}^T(\mathbf{X}_i) + \mathbf{f}(\mathbf{X}_i)\mathbf{W}\mathbf{X}_i^T + \mathbf{g}(t, \boldsymbol{\mu}_i)\mathbf{Q}\mathbf{g}^T(t, \boldsymbol{\mu}_i) \quad (9)$$

where  $\mathbf{X}_i$  is the  $n \times 2n + 1$  matrix of sigma-points and the weight vector,  $\mathbf{w}_m$ , and weight matrix,  $\mathbf{W}$ , are given by

$$\begin{aligned} \lambda &= \alpha^2(n + \kappa) - n \\ W_0^{(mean)} &= \frac{\lambda}{n + \lambda} \\ W_0^{(cov)} &= \frac{\lambda}{(n + \lambda) + (1 - \alpha^2 + \beta)} \\ W_j^{(mean)} &= \frac{1}{(2(n + \lambda))}, \quad j = 1, \dots, 2n \\ W_j^{(cov)} &= \frac{1}{(2(n + \lambda))}, \quad j = 1, \dots, 2n \\ \mathbf{w}_m &= [W_0^{(mean)} \dots W_{2n}^{(mean)}]^T \end{aligned} \quad (10)$$

$$\mathbf{W} = (\mathbf{I} - [w_m \dots w_m]) \times \text{diag} \left( W_0^{(cov)} \dots W_{2n}^{(cov)} \right) \times (\mathbf{I} - [w_m \dots w_m])^T \quad (11)$$

The constants  $\alpha$ ,  $\beta$ , and  $\kappa$  in the above equations are constant parameters of the method. The spread of sigma points is determined by  $\alpha$  and is typically a small positive value, i.e.  $1 \times 10^{-4} \leq \alpha \leq 1$ . The parameter  $\beta$  is used to incorporate prior knowledge of the distribution, and is optimally chosen as 2 for a normal distribution. The parameter  $\kappa$  can be used to exploit knowledge of the distributions higher moments, and for higher order systems choosing  $\kappa = 3 - n$  minimizes the mean-squared-error up to the fourth order. The use of the UKF in the mixture model is especially advantageous since it does not require the computation of the Jacobian matrix  $\mathbf{A}_k$ .

Notice that the weights  $w_i$  of the Gaussian components are not known at time  $t$  and must be computed as part of the solution process. To determine the unknown weights, the error in the FPKE is used as a feedback to update the weights of different Gaussian components in the mixture pdf. In other words, we seek to minimize the FPKE error under the assumption of Eqs. (3)–(6). This leads to the following optimization problem:

$$\min_{w_i(t)} J = \frac{1}{2} \int e^2(t, \mathbf{x}) d\mathbf{x}, \text{ s.t. } \sum_{i=1}^N w_i(t) = 1, \quad w_i(t) \geq 0 \quad (12)$$

Here  $e(t, \mathbf{x})$  represents the FPKE error:

$$e(t, \mathbf{x}) = \frac{\partial \hat{p}(t, \mathbf{x})}{\partial t} - \mathcal{L}_{\mathcal{FP}} \hat{p}(t, \mathbf{x}) \quad (13)$$

Again making use of the FPKE for the definition of  $\mathcal{L}_{FP}$ , and Gaussian mixture approximation of Eq. (3) for  $\hat{p}(t, \mathbf{x})$ , the cost function can be rewritten as described in Ref. [30]:

$$\min_{w_i(t')} J = \frac{1}{2} \mathbf{w}(t')^T \mathbf{M}_c \mathbf{w}(t') + \mathbf{w}(t')^T \mathbf{N}_c \mathbf{w}(t), \text{ s.t. } \mathbf{1}_{N \times 1}^T \mathbf{w}(t') = 1, \mathbf{w}(t') \geq \mathbf{0}_{N \times 1} \quad (14)$$

Here  $\mathbf{w}(t')$  represents a vector of unknown weights at time  $t + \Delta t$  while  $\mathbf{w}(t)$  represents the vector of known initial weights at time  $t$ ,  $\mathbf{1}_{N \times 1} \in \mathbb{R}^{N \times 1}$  is a vector of ones,  $\mathbf{0}_{N \times 1} \in \mathbb{R}^{N \times 1}$  is a vector of zeros and the matrices  $\mathbf{M}_c \in \mathbb{R}^{N \times N}$  and  $\mathbf{N}_c \in \mathbb{R}^{N \times N}$  are given by

$$M_{c_{ij}} = \frac{1}{\Delta t^2} |2\pi(\mathbf{P}_i + \mathbf{P}_j)|^{-1/2} \exp \left[ -\frac{1}{2} (\boldsymbol{\mu}_i - \boldsymbol{\mu}_j)^T \times (\mathbf{P}_i + \mathbf{P}_j)^{-1} (\boldsymbol{\mu}_i - \boldsymbol{\mu}_j) \right] \quad \text{for } i \neq j \quad (15)$$

$$M_{c_{ii}} = \frac{1}{\Delta t^2} |4\pi\mathbf{P}_i|^{-1/2} \quad (16)$$

$$N_{c_{ij}} = \frac{1}{\Delta t} p_{g_i} \int_V \left( \frac{\partial p_{g_j}^T}{\partial \boldsymbol{\mu}_j} \dot{\boldsymbol{\mu}}_j + \text{Tr} \left[ \frac{\partial p_{g_j}}{\partial \mathbf{P}_j} \dot{\mathbf{P}}_j \right] - \frac{1}{\Delta t} p_{g_j} + \frac{\partial p_{g_j}^T}{\partial \mathbf{x}} \mathbf{f}(t, \mathbf{x}) + p_{g_j} \text{Tr} \left[ \frac{\partial \mathbf{f}(t, \mathbf{x})}{\partial \mathbf{x}} \right] - \frac{1}{2} \text{Tr} \left[ \mathbf{g}(t, \mathbf{x}) \mathbf{Q} \mathbf{g}^T(t, \mathbf{x}) \frac{\partial^2 p_{g_j}}{\partial \mathbf{x} \partial \mathbf{x}^T} \right] \right) d\mathbf{x}, \quad p_{g_j} = \mathcal{N}(\mathbf{x}(t) | \boldsymbol{\mu}_j(t), \mathbf{P}_j(t)) \quad (17)$$

In prior work,<sup>11,26,27</sup> it is shown that the matrix  $\mathbf{M}_c$  is positive semi-definite and the cost function  $J$  is lower bounded. As a consequence of this, the aforementioned optimization problem can be posed as a convex optimization problem which is guaranteed to have a unique solution.<sup>31</sup>

A major challenge in solving this minimization problem is the need to evaluate integrals involving Gaussian pdfs over the volume  $V$  in the expression of matrix  $\mathbf{N}_c$ . These integrals can be computed exactly for polynomial nonlinearities and in general can be approximated by using a Gaussian quadrature, Monte Carlo integration or Unscented transformation.<sup>32</sup> While in lower dimensions the Unscented transformation is mostly equivalent to the Gaussian quadrature, in higher dimensions the Unscented transformation is computationally more appealing in evaluating integrals since the number of points grows only linearly with the number of dimensions. Of course there is a tradeoff; there is a loss of accuracy<sup>32</sup> in the integration, which can only be overcome by adding additional points to the summation. In Refs. [13, 30], the efficacy of the Unscented transformation in approximating these expectation integrals is demonstrated.

## B. Measurement Update for Reducing Uncertainty

The use of sensor data to correct and refine the dynamical model forecast so as to reduce the associated uncertainty is a logical improvement over purely model-based prediction. However, mathematical models for various sensors are generally based upon the ‘‘usefulness’’ rather than the ‘‘truth’’ and do not provide all the information that one would like to know. Care must be taken when assimilating the observational data.

Standard nonlinear filtering algorithms use a discrete-time process model and measurement model, given by the following equation:

$$\mathbf{y}_k = \mathbf{h}(t_k, \mathbf{x}_k) + \mathbf{v}_k, \quad \mathbf{x}_k = \mathbf{x}(t_k) \quad (18)$$

where the nonlinear function  $\mathbf{h}(\cdot)$  captures the sensor model and  $\mathbf{v}_k$  denotes the measurement noise, which is a temporally uncorrelated, zero-mean random sequence with known covariance,  $\mathbf{R}_k$ .

Roughly speaking, between two measurement time instants the procedure discussed in the last section can be used to propagate the weights, mean and covariance of different Gaussian components through a nonlinear dynamical system and whenever a measurement is available, Bayes’ rule can be used to update the conditional pdf:

$$p(\mathbf{x}_k | \mathbf{Y}_k) = \frac{p(\mathbf{y}_k | \mathbf{x}_k) p(\mathbf{x}_k | \mathbf{Y}_{k-1})}{\int p(\mathbf{y}_k | \mathbf{x}_k) p(\mathbf{x}_k | \mathbf{Y}_{k-1}) d\mathbf{x}_k} \quad (19)$$

Here,  $p(\mathbf{x}_k|\mathbf{Y}_{k-1})$  represents the prior pdf usually obtained by propagating the initial pdf through the FPKE,  $p(\mathbf{y}_k|\mathbf{x}_k)$  describes the likelihood that we observe  $\mathbf{y}_k$  given  $\mathbf{x}_k$  and  $p(\mathbf{x}_k|\mathbf{Y}_k)$  represents the posterior pdf of  $\mathbf{x}_k$ . While both the state and the covariance matrix are updated using the EKF or UKF measurement update equations, the weights are updated using the Bayes' rule:

$$\boldsymbol{\mu}_i(t_{k+1}|t_{k+1}) = \boldsymbol{\mu}_i(t_{k+1}|t_k) + \mathbf{K}_i(t_k) (\mathbf{y}_k - \mathbf{h}(t, \boldsymbol{\mu}_i(t_{k+1}|t_k))) \quad (20)$$

$$\mathbf{P}_i(t_{k+1}|t_{k+1}) = (\mathbf{I} - \mathbf{K}_i(t_k)\mathbf{H}_i(t_k))\mathbf{P}_i(t_{k+1}|t_k), \quad \mathbf{H}_i(t_k) = \left. \frac{\partial \mathbf{h}(t, \mathbf{x}_k)}{\partial \mathbf{x}_k} \right|_{\mathbf{x}_k = \boldsymbol{\mu}_i(t_{k+1}|t_k)} \quad (21)$$

$$\mathbf{K}_i(t_k) = \mathbf{P}_{k+1|k}^i \mathbf{H}_k^i \left( \mathbf{H}_k^i \mathbf{P}_{k+1|k}^i (\mathbf{H}_k^i)^T + \mathbf{R}_k \right)^{-1} \quad (22)$$

$$w_i(t_{k+1}|t_{k+1}) = \frac{w_i(t_{k+1}|t_k)\beta_k^i}{\sum_{i=1}^N w_i(t_{k+1}|t_k)\beta_k^i}, \quad \beta_k^i = \mathcal{N}(\mathbf{z}_k - \mathbf{h}(t, \boldsymbol{\mu}_i(t_{k+1}|t_k)), \mathbf{H}_i(t_k)\mathbf{P}_i(t_{k+1}|t_k)\mathbf{H}_i^T(t_k) + \mathbf{R}_k) \quad (23)$$

A quasi-optimal state estimate and corresponding error covariance matrix can be obtained by making use of the following relations:

$$\boldsymbol{\mu}_{t|k} = \sum_{i=1}^N w_i(t|t_k)\boldsymbol{\mu}_i(t|t_k), \quad \mathbf{P}_{t|k} = \sum_{i=1}^N w_i(t|t_k) [\mathbf{P}_i(t|t_k) + (\boldsymbol{\mu}_i(t|t_k) - \boldsymbol{\mu}_{t|k})(\boldsymbol{\mu}_i(t|t_k) - \boldsymbol{\mu}_{t|k})^T] \quad (24)$$

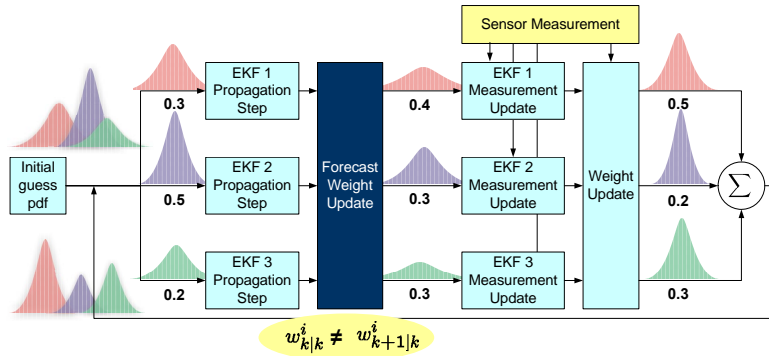


Figure 2. A Schematic of Adaptive Gaussian Sum Filter (AGSF)

Figure 2 shows the implementation scheme for the proposed nonlinear filter. An advantage of the proposed method is the decoupling of uncertainty characterization problem into many small scale linear uncertainty propagation problems. As a consequence, the algorithm can be parallelized on today's high performance computing systems.

In Refs. [11–15, 30], results have been presented comparing these new ideas with many existing methods using several benchmark problems including the spacecraft attitude estimation problem.<sup>15</sup> In all of these diverse test problems, the adaptive Gaussian mixture-based nonlinear filtering algorithm is found to produce considerably smaller errors as compared to existing methods.

### III. Entropy-Based Data Association

To develop a successively refining pdf representation, it is important to define a metric for the data association error, so that improvements due to refinements can be assessed. In this paper, an information-theoretic basis is used to quantify the target tracking error. The inspiration comes from the notion of entropy in Shannon's famous 1948 paper.<sup>33</sup> Entropy measures the average uncertainty of a random variable, i.e., it is a measure of the amount of information needed to describe a random variable. The more information is known about a random variable, the less uncertain it is, which can be interpreted as a reduction of entropy. Fundamentally, entropy is a function of the density function and can be evaluated within a probabilistic framework. If one agrees that the pdf of a random variable is a representation of uncertainty, then it is meaningful to quantify the data association error in terms of the information theoretic metrics. The idea of

using a pdf based metric is compelling given the fact that both the likelihood and posterior pdf are generally non-Gaussian in nature.

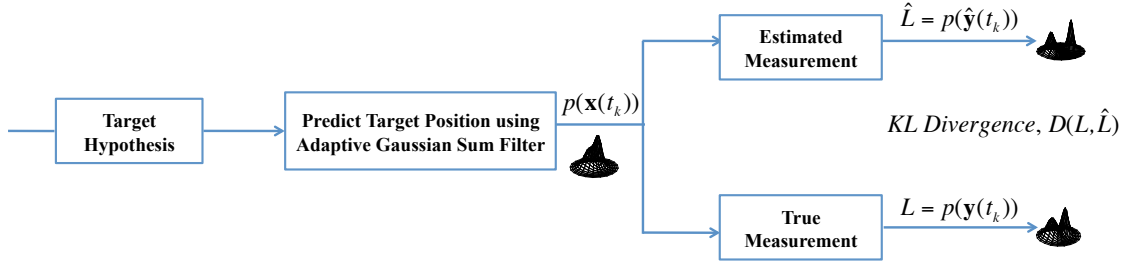


Figure 3. The KL-Divergence Based Framework for Data Association

The Shannon entropy is the most popular choice for measuring information contained in a random variable,  $\mathbf{x}$ , from its pdf  $p(\mathbf{x})$ :

$$H(\mathbf{x}) = - \int p(\mathbf{x}) \log p(\mathbf{x}) d\mathbf{x} \quad (25)$$

Kullback<sup>34</sup> and Kolmogorov<sup>35,36</sup> extended the notion of Shannon's entropy to measure the distance between two density functions. The Kullback-Leibler (KL) divergence measure, or relative entropy, describes the information geometry for the space of density functions and is defined as the ratio of the prediction error obtained with an assumed (incorrect) spectral density to the one obtained with the correct spectral density:

$$\mathcal{D}(p, q) = \int_{-\infty}^{\infty} p(\mathbf{x}) \ln \frac{p(\mathbf{x})}{q(\mathbf{x})} d\mathbf{x} = \int_{-\infty}^{\infty} p(\mathbf{x}) \ln p(\mathbf{x}) d\mathbf{x} - \int_{-\infty}^{\infty} p(\mathbf{x}) \ln q(\mathbf{x}) d\mathbf{x} \quad (26)$$

It can be shown that  $\mathcal{D}(p, q)$  is non-negative and is zero if and only if  $p = q$ . The first term in the aforementioned expression for the KL-divergence is the measure of uncertainty in the true pdf  $p$  while second term is the measure of uncertainty in  $q$  relative to the true pdf  $p$ . Also, if  $p$  is assumed to be Gaussian with covariance matrix  $\Sigma$ , then the first term can be analytically computed as:

$$\int_{-\infty}^{\infty} p(\mathbf{x}) \ln p(\mathbf{x}) d\mathbf{x} = \ln \left( \sqrt{|2\pi e \Sigma|} \right) \quad (27)$$

In Refs. [37–39] an information theoretic KL-divergence measure has been proposed to measure the confidence for fusion and tracking that has been lacking earlier in the literature.

To understand the role of the KL-divergence in data association, consider the problem of associating a measurement  $\mathbf{y}$  to one of the possible  $M$  targets. The variable  $\mathbf{x}^k$  denotes the state vector corresponding to the  $k^{th}$  target and  $p(\mathbf{x}^i)$  denotes the prior density function for the state vector  $\mathbf{x}^k$  corresponding to the  $k^{th}$  target before the measurement  $\mathbf{y}$  arrives. Here,  $p(\mathbf{x}^k)$  is parameterized by the Gaussian mixture model as described previously:

$$p(\mathbf{x}^k) = \sum_{i=1}^N w_i^k(t) \mathcal{N}(\mathbf{x}^k | \boldsymbol{\mu}_i^k(t), \mathbf{P}_i^k(t)) \quad (28)$$

Further, let us assume that  $\mathcal{L} = p(\mathbf{y}|\mathbf{x})$  represents the known likelihood function representing our confidence in the accuracy of the measurement data. Now, by propagating the prior state pdf  $p(\mathbf{x}^k)$  for each target through the measurement model of Eq. (18), we can obtain the estimated likelihood function  $\hat{\mathcal{L}}^k$  representing our confidence in the estimated measurement data assuming it belongs to the  $k^{th}$  target:

$$\hat{\mathcal{L}}^k = p(\hat{\mathbf{y}}|\mathbf{x}^k) = \sum_{i=1}^N w_i^k(t) \mathcal{N}(\mathbf{y} | \mathbf{h}(\boldsymbol{\mu}_i^k(t)), \mathbf{H}_i^k \mathbf{P}_i^k(t) \mathbf{H}_i^{kT} + \mathbf{R}) \quad (29)$$

Now, the KL-divergence metric can be used to discriminate between different targets. An interpretation of the KL-divergence is that if the pdf  $\hat{\mathcal{L}}^k$  is very unlikely, then  $\mathcal{D}(\mathcal{L}, \hat{\mathcal{L}}^k)$  is large. It should be noted that

the KL-divergence measure is essentially equivalent to a standard  $\chi^2$  test for Gaussian variables, which is commonly used in data association approaches. Therefore, the KL-divergence measure is useful for both Gaussian *and* non-Gaussian cases.

#### IV. Numerical Results

In this section, numerical results are shown validating the key ideas presented in this paper. To show the effectiveness of the proposed ideas, we consider the problem of tracking a high area-to-mass ratio (HAMR) object in a low-Earth orbit subject to nonconservative atmospheric drag. The planar equations of motion for an object in low-earth-orbit that is affected by nonconservative atmospheric drag forces are given by<sup>40</sup>

$$\begin{aligned}\ddot{x} + \frac{\mu x}{r^3} &= a_{D_x}(t, x, y, \dot{x}, \dot{y}), & a_D &= \frac{1}{2} \frac{C_d A}{m} \rho v_{rel}^2 \frac{\mathbf{v}_{rel}}{|\mathbf{v}_{rel}|} \\ \ddot{y} + \frac{\mu y}{r^3} &= a_{D_y}(t, x, y, \dot{x}, \dot{y}), & \rho &= \rho_0 e^{-\frac{(r-R_\oplus)}{h}}\end{aligned}$$

where  $C_d$  is the coefficient of drag,  $A$  is the cross-sectional area,  $m$  is the mass of the object, and  $\rho$  is the atmospheric density at a given altitude. The atmospheric density model is assumed to be an exponential model with reference density  $\rho_0$ . It is also worth noting that the  $v_{rel}$  is not the velocity state vector, but rather the velocity relative to the Earth's atmosphere.

For simulation purposes, the value of the ballistic coefficient,  $B = \frac{C_d A}{m}$ , is chosen to be 1.4 which is consistent with a HAMR object.<sup>41</sup> Perfect knowledge of system dynamics is assumed, i.e., there is no process noise in the system. The initial state-pdf is assumed to be Gaussian with the following mean and covariance:

$$\mu_0 = \begin{bmatrix} 6.6032 \times 10^6 \\ 0 \\ 0 \\ 7.7695 \times 10^3 \end{bmatrix} \quad \mathbf{P}_0 = \begin{bmatrix} 1.78 \times 10^6 & 0 & 0 & 0 \\ 0 & 2.50 \times 10^5 & 0 & 0 \\ 0 & 0 & 6.25 & 0 \\ 0 & 0 & 0 & 25 \end{bmatrix}$$

The mean of the initial pdf corresponds to a starting altitude of 225 km. The covariance matrix reflects a larger uncertainty in the radial position and the tangential velocity than in the in-track position and the radial velocity, respectively.

The initial state pdf is propagated through the orbit dynamics for a full orbit using the AGSF, UKF and the sequential Monte Carlo (SMC) method with 50,000 runs. In addition to the initial Gaussian pdf, 15 mixture components with zero weights are introduced along the principal axis of the the initial covariance matrix. Figure 4 shows the contour plots corresponding to 1% of the state pdf's peak value during various times of the orbit. As expected the effects of nonlinearities and atmospheric drag skew the state pdf, which is accurately captured by the AGSF approximation and SMC runs. It is clear that the UKF and the AGSF pdf are initially identical and remain similar for some time, however, the UKF no longer accurately represents the area of uncertainty given by the SMC samples contour at the end of one orbit. These plots clearly shows the effectiveness of the AGSF method in capturing the non-Gaussian behavior of the state pdf.

To show the effectiveness of the KL-divergence measure for data association, sensor measurements (position of a RSO) are simulated at the end of an orbit. A total of 700 Monte Carlo runs have been performed to generate different measurement data, as shown in Fig. 5(a). The blue and red contour lines in Fig. 5(a) correspond to contours for the state pdf propagated through the measurement model using the UKF and the AGSF approximations, respectively. To show the efficacy of capturing the non-Gaussian behavior, the simulated measurements are divided into four different regions (Regions 1–4) of varying degree of nonlinearity. Furthermore, measurements corresponding to false targets are also generated, denoted by Regions 5 and 6. The rest of the Monte Carlo runs correspond to the high probable region of the actual state pdf.

The KL-divergence measure is computed for both the AGSF and UKF approximated pdf by using 10,000 Gaussian quadrature points and assuming the true measurement pdf (likelihood function) to be Gaussian with standard deviation of 100 m. For notational sake, the KL-divergence measure computed by using the AGSF approximation is represented by  $d_{AGSF}$  while the one using the UKF approximation is represented by  $d_{UKF}$ . Figure 5(b) shows plots for both  $d_{AGSF}$  and  $d_{UKF}$  for different Monte Carlo runs of simulated measurements. As expected the value of  $d_{AGSF}$  is consistently less than the value for  $d_{UKF}$  for measurements

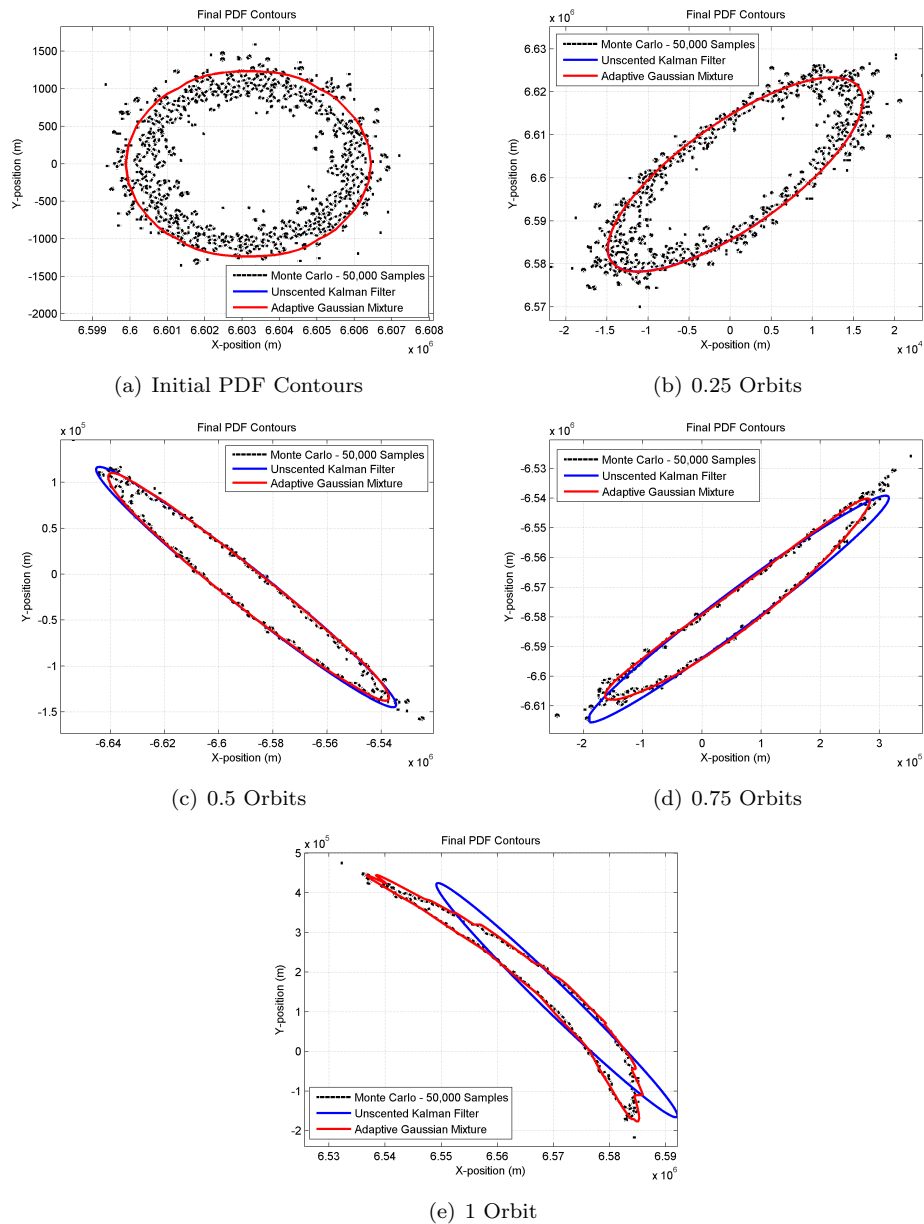
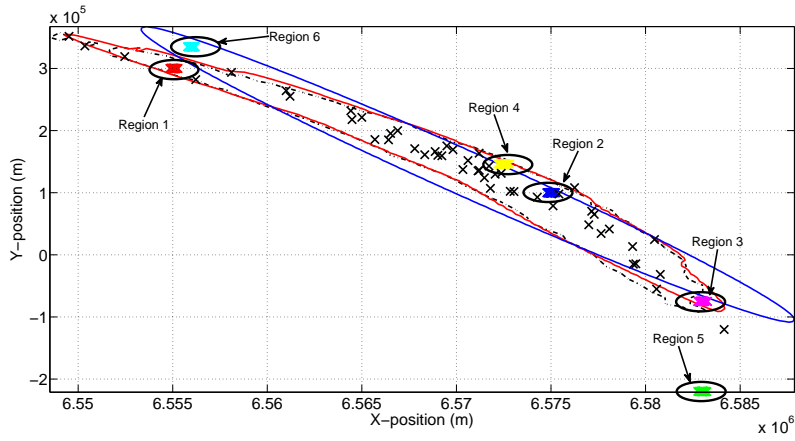
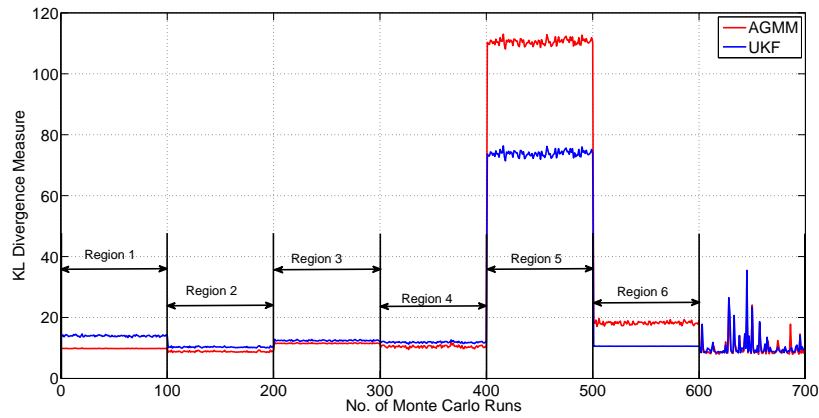


Figure 4. State pdfs Propagation for a HAMR object in a LEO Orbit with Atmospheric Drag. The blue line represents the Gaussian approximation, red line represents the Gaussian mixture approximation while black dots represent the Monte Carlo particles.

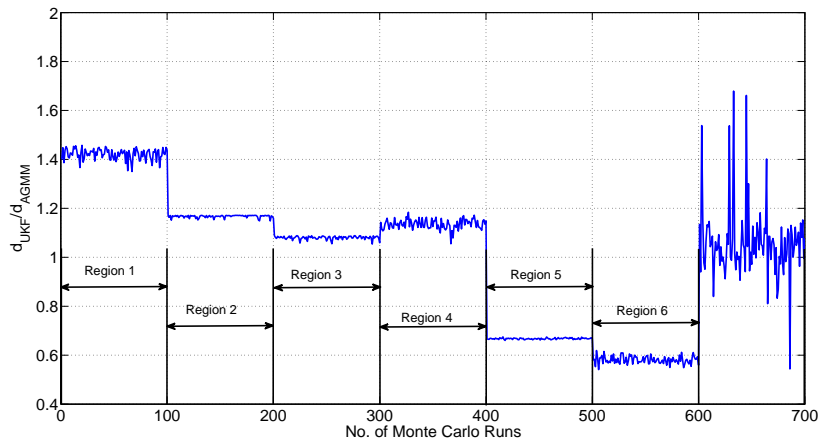
belonging to Regions 1–4 and 5. This fact is more noticeable in Fig. 5(c) which shows a plot of the ratio of the two KL-divergence measures, i.e.  $d_{AGSF}/d_{UKF}$ . Furthermore, both the UKF and AGSF correctly identify the false measurements corresponding to Region 5 by a sudden increase in the value of the KL-divergence measure, although the increase is much larger for the AGSF derived one. However, the UKF fails to identify the false measurements corresponding to Region 6 due to the skewness of the actual pdf which is not captured by the UKF. This once again illustrates the benefit of capturing the actual non-Gaussian pdf. These plots clearly illustrates the effectiveness of the AGSF and KL-divergence measure in correctly identifying targets under large uncertainty.



(a) Density Contours After One Orbit and Simulated Measurements for Different Monte Carlo Runs



(b)  $d(\mathcal{L}, \hat{\mathcal{L}})$



(c) Ratio of  $d(\mathcal{L}, \hat{\mathcal{L}})$  Computed by the AGSF and UKF

**Figure 5. Data Association Results**

## V. Conclusion

In this paper a new approach for data association of resident space object tracking was developed. The approach combines an adaptive Gaussian sum filter with the Kullback-Leibler divergence measure-based

data association metric to track space objects accurately. This approach has several advantages over existing approaches, including: it is able to approximate the pdf associated with nonlinear systems well and it is computationally efficient so that it can be executed in realtime using modern-day computers. The numerical results presented in this paper clearly provide a basis for optimism that the proposed approach can effectively work for realtime resident space object track/data association.

## VI. Acknowledgements

This work was supported by an Air Force Research Laboratory Phase I SBIR grant, FA9451-10-M-0089, under the supervision of Dr. Moriba Jah, and an Air Force Office of Scientific Research Phase I STTR grant, FA9550-10-C-0077, under the supervision of Dr. Kent Miller. The authors greatly appreciate the support.

## References

- <sup>1</sup>Chodas, P. W. and Yeomans, D. K., "Orbit Determination and Estimation of Impact Probability for Near Earth Objects," *Proceedings of the Guidance and Control*, Vol. 101 of *Advances in the Astronautical Sciences*, 1999, pp. 21–40.
- <sup>2</sup>Devis, J., Singla, P., and Junkins, J. L., "Identifying Near-term Missions and Impact Keyholes for Asteroid 99942 Apophis," 7th International Conference On Dynamics and Control of Systems and Structures in Space, London, England, July 2006.
- <sup>3</sup>Doucet, A., de Freitas, N., and Gordon, N., *Sequential Monte-Carlo Methods in Practice*, Springer-Verlag, April 2001, 6-14.
- <sup>4</sup>Iyengar, R. N. and Dash, P. K., "Study of the random vibration of nonlinear systems by the Gaussian closure technique," *Journal of Applied Mechanics*, Vol. 45, 1978, pp. 393–399.
- <sup>5</sup>Roberts, J. B. and Spanos, P. D., *Random Vibration and Statistical Linearization*, Wiley, 1990, 122-176.
- <sup>6</sup>Lefebvre, T., Bruyninckx, H., and Schutter, J. D., "Kalman Filters of Non-Linear Systems: A comparison of Performance," *International journal of Control*, Vol. 77, No. 7, 2004, pp. 639–653.
- <sup>7</sup>Daum, F. and Huang, J., "Curse of dimensionality and particle filters," *Aerospace Conference, 2003. Proceedings. 2003 IEEE*, Vol. 4, March 8-15, 2003, pp. 1979–1993.
- <sup>8</sup>Risken, H., *The Fokker-Planck Equation: Methods of Solution and Applications*, Springer, 1989, 1-12, 32-62.
- <sup>9</sup>Park, R. S. and Scheeres, D. J., "Nonlinear Mapping of Gaussian Statistics: Theory and Application to Spacecraft Design," *AIAA Journal for Guidance, Control and Dynamics*, Vol. 29, No. 6, Nov.-Dec. 2006.
- <sup>10</sup>Fuller, A. T., "Analysis of nonlinear stochastic systems by means of the Fokker-Planck equation," *International Journal of Control*, Vol. 9, 1969, pp. 6.
- <sup>11</sup>Terejanu, G., Singla, P., Singh, T., and Scott, P. D., "Uncertainty Propagation for Nonlinear Dynamical Systems using Gaussian Mixture Models," *Journal of Guidance, Control, and Dynamics*, Vol. In Press, 2008.
- <sup>12</sup>Terejanu, G., Singla, P., Singh, T., and Scott, P. D., "A Novel Gaussian Sum Filter Method for Accurate Solution to Nonlinear Filtering Problem," *2008 International Conference on Information Fusion*.
- <sup>13</sup>Giza, D. and Singla, P., "An Approach for Nonlinear Uncertainty Propagation: Application to Orbital Mechanics," *2009 AIAA Guidance Navigation and Control Conference*.
- <sup>14</sup>Terejanu, G., George, J., and Singla, P., "An Adaptive Gaussian Sum Filter For The Spacecraft Attitude Estimation Problem," *F. Landis Markley Astronautics Symposium*, Cambridge, MD, June, 2008.
- <sup>15</sup>Terejanu, G., George, J., and Singla, P., "An Adaptive Gaussian Sum Filter For The Spacecraft Attitude Estimation Problem," *Accepted for publication in the Journal of Astronautical Sciences*, May, 2009.
- <sup>16</sup>Karlsson, R. and Gustafsson, F., "Monte Carlo Data Association for Multiple Target Tracking," *Target Tracking: Algorithms and Applications (Ref. No. 2001/174)*, Vol. 1, 2001, pp. 13/1–13/5.
- <sup>17</sup>Frank, O., Nieto, J., Guivant, J., and Scheduling, S., "Multiple Target Tracking Using Sequential Monte Carlo Methods and Statistical Data Association," *International Conference on Intelligent Robots and Systems*, 2003, pp. 2718–2723.
- <sup>18</sup>Vermaak, J., Godsill, S. J., and Perez, P., "Monte Carlo Filtering for Multi-Target Tracking and Data Association," *Transactions on Aerospace and Electronic Systems*, Vol. 41, No. 1, Jan. 2005, pp. 309–332.
- <sup>19</sup>Hue, C., Le Cadre, J. P., and Perez, P., "Sequential Monte Carlo Methods for Multiple Target Tracking and Data Fusion," *Transactions on Signal Processing*, Vol. 50, No. 2, Feb. 2002, pp. 309–325.
- <sup>20</sup>Khan, Z., Balch, T., and Dellaert, F., "MCMC-Based Particle Filtering for Tracking a Variable Number of Interacting Targets," *IEEE Transactions on Pattern Analysis and Machine Intelligence*, Vol. 27, No. 11, Nov. 2005, pp. 1805–1819.
- <sup>21</sup>Lambert, H. C., Daum, F. E., and Weatherwax, J. L., "A Split-Step Solution of the Fokker-Planck Equation for the Conditional Density," *Signals, Systems and Computers, 2006. ACSSC '06. Fortieth Asilomar Conference on*, Oct.-Nov. 2006, pp. 2014–2018.
- <sup>22</sup>Kumar, M., Singla, P., Chakravorty, S., and Junkins, J. L., "A Multi-Resolution Approach for Steady State Uncertainty Determination in Nonlinear Dynamical Systems," *38th Southeastern Symposium on System Theory*, 2006.
- <sup>23</sup>Kumar, M., Singla, P., Chakravorty, S., and Junkins, J. L., "The Partition of Unity Finite Element Approach to the Stationary Fokker-Planck Equation," *2006 AIAA/AAS Astrodynamics Specialist Conference and Exhibit, Keystone, CO*, Aug. 21-24, 2006.

- <sup>24</sup>Muscolino, G., Ricciardi, G., and Vasta, M., "Stationary and non-stationary probability density function for non-linear oscillators," *International Journal of Non-Linear Mechanics*, Vol. 32, 1997, pp. 1051–1064.
- <sup>25</sup>Paola, M. D. and Sofi, A., "Approximate solution of the Fokker-Planck-Kolmogorov equation," *Probabilistic Engineering Mechanics*, Vol. 17, 2002, pp. 369–384.
- <sup>26</sup>Terejanu, G., Singla, P., Singh, T., and Scott, P. D., "Uncertainty Propagation for Nonlinear Dynamical Systems using Gaussian Mixture Models," *Proceedings of the AIAA Guidance, Navigation and Control Conference and Exhibit*, Honolulu, HI, 2008.
- <sup>27</sup>Singla, P. and Singh, T., "A Gaussian function Network for Uncertainty Propagation through Nonlinear Dynamical System," *18th AAS/AIAA Spaceflight Mechanics Meeting, Galveston, TX*, Jan. 27-31, 2008.
- <sup>28</sup>Alspach, D. and Sorenson, H., "Nonlinear Bayesian estimation using Gaussian sum approximations," *Automatic Control, IEEE Transactions on*, Vol. 17, No. 4, 1972, pp. 439–448.
- <sup>29</sup>Sarkka, S., "On Unscented Kalman Filtering for State Estimation of Continuous-Time Nonlinear Systems," *Automatic Control, IEEE Transactions on*, Vol. 52, No. 9, 2007, pp. 1631–1641.
- <sup>30</sup>Terejanu, G., Singla, P., Singh, T., and Scott, P. D., "Decision Based Uncertainty Propagation Using Adaptive Gaussian Mixtures," *2009 International Conference on Information Fusion*.
- <sup>31</sup>Boyd, S. and Vandenberghe, L., *Convex Optimization*, Cambridge University Press, 2004, 67-78, 152-159.
- <sup>32</sup>Honkela, A., "Approximating nonlinear transformations of probability distributions for nonlinear independent component analysis," *IEEE International Joint Conference on Neural Networks*, 2004.
- <sup>33</sup>Shannon, C. E., "A mathematical theory of communication," *Bell System Tech. J.*, Vol. 27, 1948, pp. 379–423, 623–656.
- <sup>34</sup>Kullback, S. and Leibler, R., "On Information and Sufficiency," *Ann. Math. Stat.*, Vol. 22, 1951, pp. 79–86.
- <sup>35</sup>Kolmogorov, A. N., "On the Shannon theory of information in the case of continuous signals," *IRE Trans. Inform. Theory*, Vol. 2, 1956, pp. 102–108.
- <sup>36</sup>Kolmogorov, A. N., *Information Theory and the Theory of Algorithms*, Vol. III of *Selected Work of A. N. Kolmogorov*, Kluwer Academic Publisher, Moscow, 1987.
- <sup>37</sup>Liggins, II, M. E., Nebrich, M. A., and Chang, K. C., "Information theoretics for improved tracking and fusion performance," *Society of Photo-Optical Instrumentation Engineers (SPIE) Conference Series*, edited by I. Kadar, Vol. 5096 of *Society of Photo-Optical Instrumentation Engineers (SPIE) Conference Series*, Aug. 2003, pp. 379–386.
- <sup>38</sup>Xu, Y., Tan, Y., Lian, Z., and He, R., "An information theoretic approach based Kullback-Leibler discrimination for multiple target tracking," *Information and Automation, 2009. ICIA '09. International Conference on*, June 2009, pp. 1129–1134.
- <sup>39</sup>Berry, P. E. and Fogg, D. A. B., "GAMBIT: Gauss-Markov and Bayesian Inference Technique for Information Uncertainty and Decision-making in Surveillance Simulations," .
- <sup>40</sup>Vallado, D. A., *Fundamentals of Astrodynamics and Applications*, Microcosm, 2007.
- <sup>41</sup>T. Schildknecht, R. Musci, T. F., "Properties of the high area-to-mass ratio space debris population at high altitudes," *Advances in Space Research*, Vol. 41, 2008, pp. 1039–1045.